Maternal expression of the novel centrosome assembly factor Wdr8 is required for vertebrate embryonic mitosis and development

Daigo Inoue[1], Manuel Stemmer[1], Thomas Thumberger[1], Joachim Wittbrodt[1], and Oliver J. Gruss[2]

[1]Centre for Organismal Studies (COS), Im Neuenheimer Feld 230, 69120 Heidelberg, Germany, [2]Zentrum für Molekulare Biologie der Universität Heidelberg (ZMBH), DKFZ-ZMBH Alliance, Im Neuenheimer Feld 282, 69120 Heidelberg, Germany.

Abstract

The assembly of the first centrosome occurs upon fertilisation when the male centrioles recruit pericentriolar material (PCM) from the egg cytoplasm. While inaccuracy in the assembly of centrosomes leads to infertility and abnormal embryogenesis, the mechanism that ensures accurate assembly in vertebrate embryos remains obscure. Here we applied a CRISPR-Cas9-mediated gene knockout to show that Wdr8, a novel centrosomal protein, is maternally essential for PCM assembly during embryonic mitoses of medaka (*Oryzias latipes*). Maternal/zygotic Wdr8-null ($Wdr8^{-/-}$) blastomeres exhibit severe defects in PCM assembly that cause them to divide asymmetrically and develop multipolar mitotic spindles and aneuploidy. We demonstrate that Wdr8 interacts via its WD40 domains with the centriolar satellite protein SSX2IP. Strikingly, exogenously provided Wdr8 fully rescues $Wdr8^{-/-}$ embryos to adulthood, except in variants with mutations in the WD40 domains. This combination of targeted gene inactivation and *in vivo* reconstitution of the maternally essential Wdr8-

SSX2IP complex reveals an essential link between maternal PCM and the stability of the zygotic genome in the early vertebrate embryo.

Introduction

The animal microtubule organising centre (MTOC), or centrosome, comprises a pair of centrioles embedded in pericentriolar material (PCM)[1-4]. The centrosome duplicates during every cell cycle to define the two MTOCs of the bipolar mitotic spindle[2, 3]. An abnormal assembly or number of centrosomes can cause cell division failure, genomic instability and tumorigenesis in somatic cells[5-7]. Their accurate assembly, on the other hand, governs the progression of early cleavages in animal zygotes. Most animal oocytes eliminate centrosomes during oogenesis, supposedly to avoid centriole aging, parthenogenesis or abnormal embryonic mitoses with an excess number of centrosomes[3, 8, 9]. The developing oocytes accumulate maternal centrosomal factors to establish the initial zygotic centrosome upon fertilisation by assembling PCM around a paternally introduced centriole[8, 9]. This serves as a template for the numerous centrosomes that are created during subsequent cleavages. Ultimately, therefore, the success of fertilisation and embryonic development depends on the accurate assembly of the initial centrosome from paternal and maternal material during fertilisation[9].

In somatic cells in culture, bipolar mitotic spindle and metaphase progression can occur normally in the absence of the centrosome[10, 11]. In contrast, it has been suggested that centrosomes in the *Drosophila*, *C.elegans* and sea urchin zygotes are essential for embryonic mitoses (i.e. cleavages)[12-16]. For example in *Drosophila*, a PCM protein Spd-2 and a centriolar protein Sas-4 appears to be largely dispensable

for *somatic* mitosis in cultured *Drosophila* cells and later development (after midblastula transition) respectively, but is essential for embryonic mitoses via its centrosome assembly functions[15, 16, 17]. Therefore, embryonic centrosome assembly seems to require a special form of regulation involving specific maternal factors, but an analysis of the mechanisms and factors involved in this process have just begun. In contrast, surprisingly, such crucial role of the centrosome controlled by maternal centrosome factors in vertebrate embryos has been poorly understood. Undoubtedly, there is a compelling need to reveal the centrosomes' physiological roles in vertebrate embyrogenesis to provide insights into development and infertility mechanisms in humans. However, it is still elusive partly due to the difficulty of peeling apart the distinct functions of maternal and zygotic factors using the knock out methods at hand.

However, a few zebrafish mutants have served as a basis for examining the physiological functions of maternal centrosomal factors in vertebrates[18-20]. The *cellular atoll* (*cea*) embryo, a maternal-effect Sas-6 mutant, exhibits a failure of centrosome duplication, and has thus revealed functions of centrosomal factors that have been conserved in human somatic cells and teleost embryos[19]. The lymphoid-restricted membrane protein (lrmp) mutant *futile* displays a failure of the attachment of centrosomes to pronuclei immediately after fertilisation, again demonstrating a maternal-specific function[20]. But many novel factors have scarcely been investigated in vertebrates, making it impossible to model the molecular networks required for centrosome assembly during the initial stages of embryogenesis and later development.

To gain molecular insights into the role of maternal-specific centrosomal factors in centrosome assembly *in vivo*, we used the vertebrate model medaka (*Oryzias latipes*)[21]. We analysed an uncharacterized WD40 repeat containing protein, Wdr8,

(the orthologue of human WRAP73) that we recently identified in a screen for maternal proteins[22]. We applied CRISPR-Cas9-mediated targeted gene inactivation, and elicited specific centrosome assembly defects in the absence of maternal and zygotic Wdr8. This allowed us to unravel an essential role for Wdr8 in maternal PCM assembly. Subsequently we used mRNA injection, which mimics maternal gene expression, and observed a remarkable reconstitution of centrosome assembly, proper cell divisions and gross development until adulthood. This *in vivo* reconstitution strategy of maternal Wdr8 functions allowed us to perform a straightforward screening of mutant variants that revealed domains/modules of the Wdr8 protein essential for PCM assembly in living vertebrate embryos. Overall, this system clearly delivered molecular insights into Wdr8's essential function in embryonic centrosome assembly.

Maternal but not paternal Wdr8 is essential for symmetric cleavages of Medaka embryos

In a recent study we identified a number of proteins that were specifically upregulated in *Xenopus laevis* oocytes. Alongside the centrosome assembly factor SSX2IP[22], our screen revealed an upregulation of Wdr8, a previously uncharacterized WD40 repeat-containing protein. Particularly interesting was the observation that the two proteins interacted with each other in *Xenopus* egg extracts (OJG, unpublished data).

To analyse Wdr8's functions in early vertebrate development, we took advantage of the transparency of medaka embryos to carry out a cell biological analysis combined with a CRISPR-Cas9 genome editing approach to target and inactivate medaka Wdr8 (OlWdr8, hereafter referred to as Wdr8). This inactivation was achieved through the targeted integration of a GFP-stop cassette into exon-3 of the

Wdr8 locus (Extended Data Fig. 1a, b). A cross of heterozygous parents yielded Wdr8$^{-/-}$ homozygous offspring that showed no obvious abnormalities during development and were phenotypically undistinguishable from wild-type fish through all stages to adulthood (Extended Data Fig. 2). However, when we compared the four combinations resulting from a cross of Wdr8$^{-/-}$ and wild-type fish (Fig. 1a), we found a severe phenotype in all embryos from homozygous mothers. All maternal/zygotic Wdr8$^{-/-}$ mutants (m/zWdr8$^{-/-}$) exhibited cleavage cycles that were significantly delayed (by 20-30 min) following the first cleavage (Fig. 1b). The second division and the following cleavage cycles revealed abnormal asymmetric cleavages with a failure of cytokinesis (Fig. 1a), which were sometimes observed during the first division (Supplementary information (SI) Movie 3). In the absence of maternally provided Wdr8, these embryos failed to gastrulate or reach the neurula stage (St.18)[23] (Fig. 1a) . In contrast, the development of all embryos from homozygous fathers was indistinguishable from that wild-type embryos (Fig. 1a and Extended Data Fig. 3). These results demonstrate that maternally provided Wdr8 is essential for faithful cleavages in the large blastomeres of the early fish embryo.

Exogenous expression of Wdr8 can efficiently rescue Wdr8$^{-/-}$ zygotes

Given these indications that the presence of maternal Wdr8 during cleavage divisions suffices for the progression of normal development, we next performed rescue experiments in the maternal/zygotic mutants (Wdr8$^{-/-}$). We injected mRNA encoding an EYFP-fusion of the human WDR8/WRAP73 orthologue (here called EYFP-huWdr8) into m/zWdr8$^{-/-}$ zygotes within 5-10 min post fertilisation (mpf). At just 60 min after injection (about 70 mpf), functional proteins were detected from both the control mRNA, encoding EGFP alone, and EYFP-huWdr8. This was the point at

126 which embryos underwent their first cleavage. While all the Wdr8$^{-/-}$ embryos
127 injected with EGFP showed abortive development, EYFP-huWdr8 expression fully
128 rescued the cleavages and over 90 % of the injected eggs progressed through
129 gastrulation to subsequent developmental stages (Fig. 1c, d). Intriguingly, about 70%
130 of these embryos developed into juveniles indistinguishable from wild-type fish based
131 on gross morphology (data not shown). These results not only confirmed the
132 specificity of the knockout phenotype, but also clearly demonstrated that maternal
133 Wdr8 plays an essential role in early development by maintaining the integrity of
134 embryonic cleavages.
135
136 **Centrosomal localisation of Wdr8 in rescued Wdr8$^{-/-}$ zygotes**
137 The fluorescent tag of the rescue construct allowed us to determine the localisation of
138 EYFP-huWdr8 in living blastomeres. *In vivo* microscopy showed that EYFP-huWdr8
139 localised specifically to one or two distinct dot-like domains in each blastomere of the
140 rescued embryos (Fig. 2a, b). During the cleavage cycles from the one- to the four-
141 cell stage, the two domains remained adjacent to each other, then separated and
142 migrated to opposing sides of the blastomeres during mitosis (Fig. 2a and SI Movie 1).
143 At the end of mitosis (before the emergence of the cleavage furrow), the Wdr8
144 domains were more dispersed (Fig. 2a and SI Movie 1). This localisation was
145 strikingly reminiscent of the pattern that centrosomes follow during the cell cycle as
146 they separate to form mitotic spindle. Strikingly, EYFP-huWdr8 co-localised with γ-
147 tubulin as well as the centriolar satellite (CS)-marker PCM1[24,25] at both prophase and
148 metaphase, demonstrating that Wdr8 is a novel maternal centrosomal and CS factor in
149 medaka embryos (Fig. 2c). In controls (EGFP-expressing wild-type and m/zWdr8$^{-/-}$
150 blastomeres), the EGFP signal was found in the cytoplasm, confirming that the

centrosomal localisation of the EYFP-huWdr8 signal is due to the Wdr8 sequence (SI Movies 1, 2, and 3). Taken together, our results indicate that Wdr8 acts as a centrosomal organiser in embryonic mitoses.

Wdr8 is essential for PCM assembly during rapid embryonic mitoses.

The centrosomal localisation of γ-tubulin and PCM1 in the embryos rescued by EYFP-huWdr8 expression was comparable to that observed in wild-type embryos (Fig. 2d). This indicates that EYFP-huWdr8 successfully rescues the phenotype of $Wdr8^{-/-}$ embryos by restoring the function of embryonic MTOCs. We therefore asked if MTOC assembly is affected in m/z$Wdr8^{-/-}$ blastomeres. At prophase and metaphase in these blastomeres, γ-tubulin and PCM1 were severely scattered compared to the wild-type, sometimes forming multiple PCM foci that were unevenly fragmented (Fig. 3a). Furthermore, while bipolar mitotic spindles readily formed in wild-type blastomeres, the scattered PCM of m/z$Wdr8^{-/-}$ blastomeres induced multipolar spindle assembly from prophase to telophase (Fig. 3b and Extended Data Fig. 4a, b). Importantly, these centrosomal and spindle abnormalities led to severe chromosomal instability (Fig. 3a, b and Extended Data Fig. 4a, b). In contrast, blastomeres expressing exogenous EYFP-huWdr8 recovered from all three defects: abnormal PCM assembly, multipolar spindle formation and aneuploidy (Fig. 2c and Fig. 3b). These results demonstrate that maternal Wdr8 ensures faithful PCM assembly and is essential for the maintenance of functional MTOCs in embryonic mitosis.

The WD40 domains of Wdr8 are essential for both localisation and function of Wdr8

The fact that exogenously provided Wdr8 mRNA effects a highly efficient rescue during early cleavage stages provides a clear, systematic approach to the identification of interaction partners and the domains of Wdr8 that permit them to bind. Wdr8 is conserved across species from yeast to humans, and vertebrates exhibit four WD40 domains (Fig. 4a). WD40 domains are often involved in protein-protein interactions[26], suggesting that they might play an important role in Wdr8's function. We selected amino acids in the WD40 domains of Wdr8 that were conserved across species and mutated either W196D197 (WD40_1) or W359D360 (WD40_3) by Alanine (hereafter each mutant variant called 196/197AA and 359/360AA, Fig. 4a). To assess the functional relevance of the WD40 domain, we performed a rescue assay by injecting mRNA into m/zWdr8$^{-/-}$ zygotes. mRNAs of all the variants (EYFP-huWdr8 wild-type, EYFP-196/197AA, or EYFP-359/360AA) were expressed at similar levels (Extended Data Fig. 5 and 359/360AA, data not shown). In contrast to the wild-type construct, Wdr8 lost its centrosomal localisation in both WD mutant variants and was mainly detected in the cytoplasm (Fig. 4b).

When blastomeres entered mitosis, a weak but visible centrosomal localisation of the mutant variants was observed in live imaging of either EYFP-196/197AA- or EYFP-359/360AA-injected embryos (Fig. 4c, SI Movie 4, time points at 08:11, 53:12, and 98:12). Individual blastomeres exhibited multiple foci, but they disappeared during the subsequent cleavage cycles (Fig. 4c, SI Movie 4). Interestingly, in m/zWdr8$^{-/-}$ blastomeres, both WD variants were ubiquitously dispersed throughout the cytoplasm and slightly co-localised with scattered γ-tubulin and PCM1 at prophase (Fig. 4d). This indicates that WD variants are hypomorphic forms of Wdr8 that inefficiently localise to the centrosome, and demonstrates that the WD40 domain is essential for proper PCM/CS assembly.

Importantly, abnormal PCM/CS assembly led to multipolar spindles as well as chromosomal instability (Fig. 4e). This was consistent with the finding that neither of the WD mutant variants was able to rescue the early m/zWdr8$^{-/-}$ phenotypes or their subsequent abortive development (Fig. 4b). In contrast, the mutation of four conserved putative Cdk1-phosphorylation motifs (mutations substituting AP for SP, a site S232 lies in WD40_2)[27], affected neither the localisation nor the rescue function of Wdr8 in m/zWdr8$^{-/-}$ embryos (data not shown). These results clearly demonstrate that intact WD40 domains govern the centrosomal localisation of Wdr8 and are required for proper PCM/CS functions in early embryonic mitoses of cleavage stages.

The WD40 domains of the Wdr8-SSX2IP complex are essential specifically for its localisation and functions

We next took advantage of the mRNA-based *in vivo* reconstitution assay to address the molecular mechanisms underlying Wdr8's function. We hypothesised that WD40 domains serve either as centrosome-targeting domains or as modules for interactions with other proteins. We first tested whether the rescue of m/zWdr8$^{-/-}$ zygotes by WD variants was achieved by targeting them to the centrosome. We used the centrosome-targeting motif PACT to facilitate the accumulation of WD mutant variants at the centrosome[28]. Both PACT fusion constructs weakly localised to the centrosome in some embryos (Fig. 5a, PACT-359/360AA, data not shown). In these embryos, however, the embryonic lethality introduced by Wdr8 knockout was not rescued (1dpf in Fig. 5a, PACT-359/360AA, data not shown). This failure – even when Wdr8 was localised to the centrosome – strongly suggests that the WD40 domains of Wdr8 are not simply centrosome-targeting domains.

Next we tested whether WD40 domains are important for interactions with other proteins. Since Wdr8 had initially been identified as an interaction partner of the CS protein SSX2IP, we hypothesised that WD40 domains might be critical for Wdr8's interaction with SSX2IP or other centrosomal or CS proteins. To retrieve amounts of the proteins sufficient to analyse protein-protein interactions, we carried out a biochemical analysis of *Xenopus laevis* egg extracts. Following the expression of either 2xFlag-huWdr8 wild-type (WT), 2xFlag-196/197AA (196/197AA) or 2xFlag-359/360AA (359/360AA) in cytostatic factor (CSF) egg extracts arrested at metaphase[29], we performed Flag immunoprecipitations to analyse the proteins that co-precipitated. Strikingly, mass spectrometry analysis revealed that SSX2IP interacted with WT, whereas it was unable to interact with either 196/197AA or 359/360AA (Fig. 5b), clearly demonstrating that WD40 domains are essential for the Wdr8-SSX2IP interactions.

Intriguingly, although γ-tubulin was severely scattered in Wdr8$^{-/-}$ blastomeres, γ-tubulin and all the γ-TuRC subunits (including its regulatory protein Nedd1)[30-32] interacted equivalently with WT and WD variants, indicating that WD40 domains are not required for Wdr8-γ-TuRC/Nedd1 interactions (Fig. 5b). Consistent with this finding, Western blot analysis confirmed that only WT, but not WD mutant variants, interacted with SSX2IP (Fig. 5c). On the other hand, γ-tubulin's interaction with Wdr8 was independent of WD40 domains (Fig. 5c). Taken together, these results revealed that WD40 domains are the basis of the complex formed by Wdr8 with SSX2IP, but its interactions with γ-TuRC are independent of the domains. In medaka blastomeres, Wdr8 wild-type almost completely co-localised with SSX2IP, strongly suggesting that Wdr8 is a CS protein which forms a complex with SSX2IP (Fig. 5d). In contrast, SSX2IP was remarkably dispersed in the cytoplasm in both 196/197AA- and

359/360AA-expressing blastomeres (Fig. 5d, 359/360AA, data not shown), indicating that the interaction between Wdr8 and SSX2IP is crucial for mutual localisation and the function of Wdr8-SSX2IP as a CS protein complex (Fig. 5d, e).

In summary, these results clearly demonstrate that the Wdr8-SSX2IP complex is maternally essential for PCM assembly to ensure rapid embryonic mitoses.

Discussion

Although it has long been suggested that centrosomes in vertebrate is absolutely essential for embryonic mitosis, the ultimate impact of centrosomes on vertebrate embryonic development and its molecular mechanism has been ill-defined. In this study, we for the first time reveal the detailed molecular mechanism of centrosome assembly specifically regulated by the novel maternal centrosomal protein Wdr8 during medaka embryonic mitoses (Fig. 5e). Centrosomes regulated by maternal Wdr8 are absolutely essential for mitotic spindle bipolarity and accurate inheritance of the zygote genome, which is distinct from a certain dispensability of centrosomes in somatic cells (Fig. 5e). Therefore, we here present a first major step toward solving the long-standing problems of physiological significance of centrosomes in early vertebrate development.

Several studies in vertebrate embryos have explored the regulation of the centrosome during embryonic mitoses[18-20, 33, 34]. A few zebrafish maternal-effect mutants, such as *cea* (Sas-6) or *futile* (Lrmp), have revealed functions in centrosomal regulation in the embryo[19, 20]. However, these studies failed to reveal further molecular insights due to the lack of precise gene targeting and the immense efforts of forward genetic screens for maternal genes in vertebrate models. Our CRISPR-Cas9 knockout medaka line clearly segregates the distinct functional contributions of

maternal and zygotic Wdr8 during development. We show that early lethality of $Wdr8^{-/-}$ embryos can be rescued with high efficiency either through maternal effects or the exogenous expression of a functional Wdr8 mRNA, which mimics the presence of a corresponding maternal mRNA. Strikingly, the rescued animals exhibited normal development and grew to become fertile adults. This reliable "reconstitution" rescue system, based on wild-type Wdr8 or several mutant variants, provides an unambiguous readout that directly links the molecular features of Wdr8 structure to its function and interactions with SSX2IP. This indicates that reverse genetic approaches with the CRISPR-Cas9 system are ideally suited to dissect maternal- and zygotic-specific aspects of centrosome regulation, which have been lacking for vertebrate systems.

Very recently, Wdr8 was shown to form a ternary complex with SSX2IP and the minus-end-directed kinesin Pkl1 (kinesin-14 homologue), which maintains minus-end pulling forces of microtubules (MTs) in fission yeast[35]. The SSX2IP-Wdr8-Pkl ternary complex itself is required for its localisation/function in the spindle pole body (SPB)[35]. The yeast complex provides a model case in which Wdr8-SSX2IP contributes to the generation of a pulling force by the MTs at the SPB, possibly by capping γ-tubulin[35, 36]. However, the question of whether Wdr8's functions have been conserved through evolution has yet to be addressed. In cell culture, a Wdr8 partner, SSX2IP is shown to be required in CS for the recruitment of γ-tubulin ring complexes (γ-TuRCs) and other specific components into the PCM for the assembly of expanded mitotic PCM[22, 37]. While SSX2IP is not absolutely essential for the mitotic spindle bipolarity and metaphase progression in cultured cells[22, 37], its function originally identified as maternal protein from *Xenopus* eggs has not been addressed. By unveiling the exclusive function of maternal Wdr8, our data show that Wdr8 interacts

299 with SSX2IP via its WD40 domains and that this complex is essential for their mutual
300 centrosome localisation/function in medaka embryonic mitosis. Although mass
301 spectrometry analysis in our experiments could not identify kinesin-14 in either
302 SSX2IP- or Wdr8-IP samples, the localisation of SSX2IP is dependent on dynein at
303 least in *Xenopus* egg extracts[22]. Therefore, a complex of Wdr8-SSX2IP bound to
304 dynein as a minus-end-directed motor could be a highly conserved molecular module
305 whose function is crucial to ensure proper PCM assembly and maintain its structure
306 during embryonic mitosis. Since SSX2IP is exclusive to CS[22, 37], Wdr8-SSX2IP might
307 be first recognised as a cargo by dynein at the CS granule to transport the complex,
308 together with other PCM components, to the centrosome (Fig. 5e). The formation of
309 the Wdr8-SSX2IP complex via WD40 domains may therefore be a critical step in the
310 assembly of PCM components and the initiation of centrosome maturation (Fig. 5e)[38,
311 39]. Intriguingly, our mass spectrometry analysis further demonstrates that Wdr8 also
312 associates with all the γ-TuRC subunits, including its regulatory protein Nedd1, in a
313 manner independent of WD40 domains (Fig. 5b). It is plausible that Wdr8 alone could
314 serve as a platform for γ-TuRC/Nedd1 in either its transport to the centrosome or in
315 stabilising the minus-end of MT.

316 Defects of the assembly of the centrosome after fertilisation have been directly
317 linked to infertility and abnormal embryonic development in humans[40, 41]. So far the
318 causes of infertility have mainly been attributed to the abnormalities of the sperm
319 centriole[40, 41]. The effects of maternal centrosomal factors in oocytes have not yet
320 received much attention. Considering that genomic instability in aging eggs causes
321 infertility[42, 43], it is possible that the downregulation or absence of maternal
322 centrosomal factors during meiosis may contribute to infertility as well. Since Wdr8 is
323 a critical maternal factor for genomic stability as well as centrosome assembly, the

function of Wdr8 in relation to other interaction partners during meiosis needs to be addressed. On the other hand, the rescue of $Wdr8^{-/-}$ embryos through either maternal effects or an introduction of exogenous Wdr8 expression causes them to undergo normal development, which suggests that zygotic Wdr8 is dispensable for later development (Extended Data Fig. 2, 3 and, Fig.1a, c). It is possible, of course, that zygotic Wdr8 does have functions in later development beyond its role in PCM assembly, or their failure to produce a clear phenotype might be attributable to the presence of other, redundant factors.

Methods

Husbandry of fish and preparation of medaka zygotes. Husbandry of fish and preparation of zygotes were routinely performed as described previously[44]. The husbandry and all the experiments were performed according to local animal welfare standards (Tierschutzgesetz §11, Abs. 1, Nr. 1, husbandry permit number 35–9185.64/BH Wittbrodt and mutagenesis permit number G-206/09) and in accordance with European Union animal welfare guidelines. The fish facility is under the supervision of the local representative of the animal welfare agency.

Construction of CRISPR/Cas9 materials and generation of Wdr8 knockout medaka line. With CCTop (http://crispr.cos.uni-heidelberg.de)[45], a sgRNA was chosen to target exon-3 of *Oryzias latipes* Wdr8 (OlWdr8, NCBI reference sequence: XM_004070359.2) with least potential off-target sites in the remainder of the genome (Extended Data Table 1). Synthetic sgRNA oligos were annealed and cloned into pDR274 (addgene, #42250). Wdr8-sgRNA forward (5'-TAGGTCTCTCGAGCAGCCGGAC-3') Wdr8-sgRNA reverse (5'-AAACGTCCGGCTGCTCGAGAGA-3'). The donor plasmid was created as

described previously[45, 46] via Golden GATEway cloning comprising the following sequences: 1) a specific sgRNA target site derived from GFP for *in vivo* linearisation of the donor vector (cf sgRNA-1 in [45]), 2) a 665 bp homology flank corresponding to the upstream genomic sequence of the Wdr8-sgRNA target site, 3) a *GFP* variant (*GFP*^{var})[46] that was silently mutated to prevent CRISPR/Cas9-mediated cleavage by the donor-linearising sgRNA (see [45]), 4) followed by a triple polyadenylation signal. The homology flank was cloned from Cab genomic DNA with primers: Forward (5'-GCCGGATCCATGGTCCTCAGACTCCCTGT-3'), Reverse (5'-GCCGGTACCCGGCTGCTCGAGTGACCACACCT-3') to facilitate cloning into the Golden GATEway entry vector, the forward and reverse primers were extended with a BamHI or KpnI restriction site, respectively. To knock out OlWdr8, *GFP*^{var} with stop codon was inserted by homology directed repair (HDR) to generate nonsense mutation, which resulted in the C-terminal deletion of roughly 500 amino acids, i.e. deletion of >75% of full-length OlWdr8. One-cell stage Medaka zygotes were co-injected with 10 ng/µl of donor plasmid, 15 ng/µl per sgRNA (Wdr8-sgRNA and sgRNA-1[45]), 150 ng/µl Cas9 mRNA diluted in nuclease free water. Founders were screened by genotype PCR (Extended Data Fig.1b) with FinClip protocol[47] since *GFP*^{var} expression could hardly be detected, possibly due to impaired protein folding of *GFP* fused with N-terminal short fragment of OlWdr8. To achieve reproducible genotype PCR results, the program and the primer sets for the screening were fixed as below. The primers: for wild-type locus, forward (5'-AGTGTTCAAGCAGTCCAACCA-3') and reverse (5'-TGAGGAGACTAGTCCAATTGAGC-3'), for *GFP*^{var} insertion, forward (5'-AGTGTTCAAGCAGTCCAACCA-3') and reverse (5'-GAACTTGTGGCCGTTTACGT-3'). The genotype PCR reaction with Taq

polymerase (NEB): 1. 95°C for 1min, 2. 95 °C for 30s, 3. 65 °C for 30s, 4. 72 °C for 40s, repeated the cycle from step 2, 30 cycles. Heterozygous F1 fish were crossed with Cab. Heterozygous F2 fish were crossed with each other to generate F3 homozygous fish, which developed normally and grew to viable and fertile adults. By crossing F3 homozygous parents, the maternal effect of $Wdr8^{-/-}$ homozygous zygotes (F4) was obtained to analyse the function of maternal Wdr8.

Whole mount *in situ* hybridisation with medaka embryos. For whole mount *in situ* hybridisation (WISH), a full-length OlWdr8 cDNA was isolated from cDNA library of wild-type embryos (St. 32)[23], and then cloned into pGEM-T easy vector (Promega) to generate the antisense and the sense RNA probes. WISH was performed as described previously[44]. The pictures were taken under Nikon SMZ18 binocular microscope with the NIS-Elements F4.00.00 imaging software (Nikon).

Preparation of cDNAs, mRNAs, and sgRNAs. EYFP-huWdr8, 2xFlag-huWdr8, and their mutant variants were cloned into $pCS2^{+}$ for mRNA generation. WD40 mutant variants, 196/197AA and 359/360AA, were generated by mutation PCR. To create PACT fusion construct, PACT domain (kindly provided by Elmar Schiebel, Zentrum für Molekulare Biologie der Universität Heidelberg (ZMBH), Heidelberg, Germany) was cloned and N-terminally fused immediate after a WD mutant variant by fusion PCR. mRNAs were transcribed with SP6 mMessegae mMachine kit (Life technologies). sgRNAs were transcribed with mMessage mMachine T7 Ultra kit (Life technologies).

Whole mount fluorescent immunostainings with medaka blastomeres. Whole mount fluorescent immunostainings were performed with 4hpf medaka blastomeres (St. 8) as described previously[44], except for omission of the heating step, with anti-γ-tubulin (1:200 dilution, Sigma-Aldrich, T6557), anti-PCM1 (rabbit, 1:300 dilution, a

399 gift from A. Merdes, Université de Toulouse, Toulouse, France), anti-α-tubulin (1:100
400 dilution, Sigma-Aldrich, T9026), and anti-GFP (1:300 dilution, Life technologies,
401 A10262) antibodies. Secondary antibodies were Alexa Fluor 488 anti-mouse IgG
402 (Life technologies), Alexa Fluor 488 anti-chicken IgY (Life technologies), Alexa
403 Fluor 546 goat anti-mouse IgG (Life technologies), Dylight 549 goat anti-rabbit IgG
404 (Jackson ImmunoResearch), and Alexa Fluor 647 goat anti-rabbit IgG (Life
405 technologies). All secondary antibodies were incubated at 1:200 dilutions. DNA was
406 counterstained with DAPI (1:200 dilution from 5mg/ml stock, Sigma-Aldrich, D9564).
407 Images were taken with the confocal microscopy (Leica TCS SPE) with either 20x
408 water (Leica ACS APO 20x/0.60 IMM CORR) or 40x oil (Leica ACS APO 40x/1.15
409 Oil CS 0.17/E, 0.27) objectives and processed with Image J. For SSX2IP detection,
410 100 ng/μl anti-xlSSX2IP antibody was injected into one-cell stage of medaka zygotes,
411 and then subjected to immunostaining as described previously[22].
412 **Live imaging of medaka embryos.** Fluorescence in injected medaka embryos was
413 checked at 70-90 min post injection. The embryo with chorion was incubated in 3%
414 methyl cellulose/1xERM with the glass bottom dishes (MaTeck corporation). Live
415 imaging was performed by Leica SPE confocal microscope with 20x water objective.
416 Images were taken every 37s-49s (Movie 1-4) with a 2-3 μm- z-step size. Maximum
417 z-stack projection images were processed with Image J and then converted to Quick
418 Time movie files.
419 **Rescue experiments by injection of either EYFP-huWdr8 mRNA or its**
420 **individual mutant variants' mRNA.** Wdr8$^{-/-}$ fertilised eggs were immediately
421 collected after checking mating, and injected with mRNA within 5-10 min post
422 fertilisation in the precooled 0.5x ERM medium. 100 ng/μl of mRNA of either EYFP-
423 huWdr8 or its individual mutant variants was injected into Wdr8$^{-/-}$ zygotes at about

1/3 volume of one-cell stage. These zygotes were incubated in 0.5x ERM at 28 °C. Embryos at 4 hpf (St. 8) were fixed with 4% PFA in 1x PTw to perform whole mount fluorescent immunostainings. Images of external phenotypes of live embryos were taken under Nikon SMZ18 binocular microscope with the NIS-Elements F4.00.00 imaging software (Nikon).

Western blot analysis of medaka embryos at morula stage. 400 ng/µl of mRNA encoding either EYFP-huWdr8 or WD mutant variant was injected into one-cell stage zygotes. The embryos were incubated for 28 °C for 2h, and then treated with hatching enzyme for another 2h to remove chorion. 50 embryos (around St. 8) for each were softly homogenised with 100 µl cold PBS to remove the yolk. After centrifugation at 3,000 rpm for 2 min at 4 °C, the supernatant was removed and the pellet of embryos was frozen at liq N_2 and stored at -80 °C. The pellet was lysed on ice with 25 µl RIPA buffer (50 mM Tris-HCl at pH 8.0, 150 mM NaCl, 5 mM EDTA, 15 mM $MgCl_2$, 1% Triton-X100) containing 10 µM pepstatin, 10 µg/ml aprotinin, 0.1 mM PMSF, 1 mM Na_3VO_4, and 1 mM NaF. After centrifugation at 14,000 rpm for 5 min at 4 °C, 20 µl supernatant was mixed with the equal volume of 2x Laemmli sample buffer containing 10% 2-mercaptoethanol, and boiled for 10 min at 100 °C, subjected to SDS-PAGE.

Immunoprecipitation of 2xFlag-huWdr8 from *Xenopus* CSF egg extracts. *Xenopus* CSF egg extracts were routinely prepared as previously described[48]. 80 µl of the extracts was incubated with 3 µg mRNA of either 2xFlag-huWdr8 wild-type, 2xFlag-196/197AA, or 2xFlag-359/360AA for 90 min at 23 °C to express Flag-tagged fusion proteins in the extracts. The immunoprecipitations were performed with 2 µg of either anti-Flag antibody (Sigma-Aldrich, F1804) or normal mouse serum (Invitrogen, #1410) for 45 min at 23 °C, followed by incubation with 20 µl of Protein

G Sepharose 4 Fast Flow (GE Healthcare Life Sciences) slurry (in CSF-XB) for another 25 min at 23 °C by tapping every 5 min. The Protein G Sepharoses were washed twice and one time with 250 µl of TBS-T (10 mM Tris-HCl at pH7.5, 0.5% tween-20, 150 mM NaCl) and 250 µl of TBS (10 mM Tris-HCl at pH7.5, 150 mM NaCl), respectively. After removing TBS, the samples were prepared with 30 µl of 2x Laemmli sample buffer containing 10% 2-mercaptoethanol, boiled for 10 min at 100 °C, subjected to Western blot and mass spectrometry analyses as described previously[22, 49].

Dimethyl labeling and mass spectrometry. For quantitative mass spectrometry analysis, comparison of control IgG pull-down and 2xFlag-huWdr8 pull-down samples were performed by after dimethyl-labelling using stable isotopes[49, 50]. Original mass spectrometry data were analysed using Proteome Discoverer 1.4 and Mascot (Matrix Science; version 2.4) as described previously[22, 49]. Identified proteins were displayed by Scaffold_4.4.3 (Proteome Software Inc.) to retrieve significantly interacted proteins with either Wdr8 wild-type or WD40 mutant variants.

References

1. Balczon, R. The centrosome in animal cells and its functional homologs in plant and yeast cells. *Int. Rev. Cytol.* **169**, 25-82 (1996).
2. Hinchcliffe, E. H. & Sluder, G. "It takes two to tango": understanding how centrosome duplication is regulated throughout the cell cycle. *Genes Dev.* **15**, 1167-1181 (2001).
3. Delattre, M. & Gonczy, P. The arithmetic of centrosome biogenesis. *J. Cell Sci.* **117**, 1619-1630 (2004).

4. Luders, J. & Stearns, T. Microtubule-organizing centres: a re-evaluation. *Nat. Rev. Mol. Cell Biol.* **8**, 161-167 (2007).

5. Kramer, A., Neben, K. & Ho, A. D. Centrosome replication, genomic instability and cancer. *Leukemia* **16**, 767-775 (2002).

6. Anderhub, S. J., Krämer, A. & Maier, B. Centrosome amplification in tumorigenesis. *Cancer Lett.* **322**, 8-17 (2012).

7. Maiato, H. & Logarinho, E. Mitotic spindle multipolarity without centrosome amplification. *Nat. Cell Biol.* **16**, 386-394 (2014).

8. Schatten, G. The centrosome and its mode of inheritance: the reduction of the centrosome during gametogenesis and its restoration during fertilization. *Dev. Biol.* **165**, 299-335 (1994).

9. Manandhar, G., Schatten, H. & Sutovsky, P. Centrosome Reduction During Gametogenesis and Its Significance. *Biol. Reprod.* **72**, 2-13 (2005).

10. Hinchcliffe, E. H., Miller, F. J., Cham, M., Khodjakov, A. & Sluder, G. Requirement of a centrosomal activity for cell cycle progression through G1 into S phase. *Science* **291**, 1547-1550 (2001).

11. Khodjakov, A. & Rieder, C. L. Centrosomes enhance the fidelity of cytokinesis in vertebrates and are required for cell cycle progression. *J. Cell Biol.* **153**, 237-242 (2001).

12. Sluder, G., Miller, F. J. & Rieder, C. L. Reproductive capacity of sea urchin centrosomes without centrioles. *Cell Motil. Cytoskeleton* **13**, 264-273 (1989).

13. O'Connell, K. F. *et al.* The C. elegans zyg-1 gene encodes a regulator of centrosome duplication with distinct maternal and paternal roles in the embryo. *Cell* **105**, 547-558 (2001).

14. Stevens, N. R., Raposo, A. A., Basto, R., St Johnston, D. & Raff, J. W. From stem cell to embryo without centrioles. *Curr. Biol.* **17**, 1498-1503 (2007).

15. Dix, C. I. & Raff, J. W. Drosophila Spd-2 recruits PCM to the sperm centriole, but is dispensable for centriole duplication. *Curr. Biol.* **17**, 1759-1764 (2007).

16. Varmark, H. *et al.* Asterless is a centriolar protein required for centrosome function and embryo development in Drosophila. *Curr. Biol.* **17**, 1735-1745 (2007).

17. Basto, R. *et al.* Flies without centrioles. *Cell* **125**, 1375-1386 (2006).

18. Dekens, M. P., Pelegri, F. J., Maischein, H. M. & Nusslein-Volhard, C. The maternal-effect gene futile cycle is essential for pronuclear congression and mitotic spindle assembly in the zebrafish zygote. *Development* **130**, 3907-3916 (2003).

19. Yabe, T., Ge, X. & Pelegri, F. The zebrafish maternal-effect gene cellular atoll encodes the centriolar component sas-6 and defects in its paternal function promote whole genome duplication. *Dev. Biol.* **312**, 44-60 (2007).

20. Lindeman, R. E. & Pelegri, F. Localized products of futile cycle/lrmp promote centrosome-nucleus attachment in the zebrafish zygote. *Curr. Biol.* **22**, 843-851 (2012).

21. Wittbrodt, J., Shima, A. & Schartl, M. Medaka--a model organism from the far East. *Nat. Rev. Genet.* **3**, 53-64 (2002).

22. Barenz, F. *et al.* The centriolar satellite protein SSX2IP promotes centrosome maturation. *J. Cell. Biol.* **202**, 81-95 (2013).

23. Iwamatsu, T. Stages of normal development in the medaka Oryzias latipes. *Mech. Dev.* **121**, 605-618 (2004).

522 24. Kubo, A., Sasaki, H., Yuba-Kubo, A., Tsukita, S. & Shiina, N. Centriolar
523 satellites: molecular characterization, ATP-dependent movement toward
524 centrioles and possible involvement in ciliogenesis. *J. Cell Biol.* **147**, 969-980
525 (1999).
526 25. Dammermann, A. & Merdes, A. Assembly of centrosomal proteins and
527 microtubule organization depends on PCM-1. *J. Cell Biol.* **159**, 255-266
528 (2002).
529 26. Li, D. & Roberts, R. WD-repeat proteins: structure characteristics, biological
530 function, and their involvement in human diseases. *Cell Mol. Life Sci.* **58**,
531 2085-2097 (2001).
532 27. Nigg, E. A. Cellular substrates of p34(cdc2) and its companion cyclin-
533 dependent kinases. *Trends Cell Biol.* **3**, 296-301 (1993).
534 28. Gillingham, A. K. & Munro, S. The PACT domain, a conserved centrosomal
535 targeting motif in the coiled-coil proteins AKAP450 and pericentrin. *EMBO*
536 *Rep.* **1**, 524-529 (2000).
537 29. Murray, A. W. Cell cycle extracts. *Methods Cell Biol.* **36**, 581-605 (1991).
538 30. Gunawardane, R. N., Martin, O. C. & Zheng, Y. Characterization of a new
539 gammaTuRC subunit with WD repeats. *Mol. Biol. Cell* **14**, 1017-1026 (2003).
540 31. Haren, L. *et al.* NEDD1-dependent recruitment of the gamma-tubulin ring
541 complex to the centrosome is necessary for centriole duplication and spindle
542 assembly. *J. Cell Biol.* **172**, 505-515 (2006).
543 32. Luders, J., Patel, U. K. & Stearns, T. GCP-WD is a gamma-tubulin targeting
544 factor required for centrosomal and chromatin-mediated microtubule
545 nucleation. *Nat. Cell Biol.* **8**, 137-147 (2006).

546 33. Uto, K. & Sagata, N. Nek2B, a novel maternal form of Nek2 kinase, is
547 essential for the assembly or maintenance of centrosomes in early Xenopus
548 embryos. *EMBO J.* **19**, 1816-1826 (2000).
549 34. Twomey, C. *et al.* Nek2B stimulates zygotic centrosome assembly in Xenopus
550 laevis in a kinase-independent manner. *Dev. Biol.* **265**, 384-398 (2004).
551 35. Yukawa, M., Ikebe, C. & Toda, T. The Msd1-Wdr8-Pkl1 complex anchors
552 microtubule minus ends to fission yeast spindle pole bodies. *J. Cell Biol.* **209**,
553 549-562 (2015).
554 36. Toya, M. *et al.* Gamma-tubulin complex-mediated anchoring of spindle
555 microtubules to spindle-pole bodies requires Msd1 in fission yeast. *Nat. Cell*
556 *Biol.* **9**, 646-653 (2007).
557 37. Hori, A., Peddie, C. J., Collinson, L. M. & Toda, T. Centriolar satellite- and
558 hMsd1/SSX2IP-dependent microtubule anchoring is critical for centriole
559 assembly. *Mol. Biol. Cell* **26**, 2005-2019 (2015).
560 38. Palazzo, R. E., Vogel, J. M., Schnackenberg, B. J., Hull, D. R. & Wu, X.
561 Centrosome maturation. *Curr. Top. Dev. Biol.* **49**, 449-470 (2000).
562 39. Woodruff, J. B., Wueseke, O. & Hyman, A. A. Pericentriolar material
563 structure and dynamics. *Phil. Trans. R. Soc. B* **369**, 20130459 (2014).
564 40. Chatzimeletiou, K., Morrison, E. E., Prapas, N., Prapas, Y. & Handyside, A. H.
565 The centrosome and early embryogenesis: clinical insights. *Reprod. Biomed.*
566 *Online* **16**, 485-491 (2008).
567 41. Hinduja, I., Baliga, N. B. & Zaveri, K. Correlation of human sperm
568 centrosomal proteins with fertility. *J. Hum. Reprod. Sci.* **3**, 95-101 (2010).

42. Schatten, H. & Sun, Q. Y. Centrosome and microtubule functions and dysfunctions in meiosis: implications for age-related infertility and developmental disorders. *Reprod. Fertil. Dev.* **27**, 934-943 (2015).

43. Hassold, T., Hall, H. & Hunt, P. The origin of human aneuploidy: where we have been, where we are going. *Hum. Mol. Genet.* **2**, R203-208 (2007).

44. Inoue, D. & Wittbrodt, J. One for all--a highly efficient and versatile method for fluorescent immunostaining in fish embryos. *PLoS One* **6**, e19713 (2011).

45. Stemmer, M., Thumberger, T., Del Sol Keyer, M., Wittbrodt, J. & Mateo, J. L. CCTop: An Intuitive, Flexible and Reliable CRISPR/Cas9 Target Prediction Tool. *PLoS One* **10**, e0124633 (2015).

46. Kirchmaier, S., Lust, K. & Wittbrodt, J. Golden GATEway cloning--a combinatorial approach to generate fusion and recombination constructs. *PLoS One* **8**, e76117 (2013).

47. Rembold, M., Lahiri, K., Foulkes, N. S. & Wittbrodt, J. Transgenesis in fish: efficient selection of transgenic fish by co-injection with a fluorescent reporter construct. *Nat. Protoc.* **1**, 1133-1139 (2006).

48. Ohe, M. *et al.* Emi2 inhibition of the anaphase-promoting complex/cyclosome absolutely requires Emi2 binding via the C-terminal RL tail. *Mol. Biol. Cell* **21**, 905-913 (2010).

49. Klinger, M. *et al.* The novel centriolar satellite protein SSX2IP targets Cep290 to the ciliary transition zone. *Mol. Biol. Cell* **25**, 495-507 (2014).

50. Boersema, P. J., Raijmakers, R., Lemeer, S., Mohammed, S. & Heck, A. J. Multiplex peptide stable isotope dimethyl labeling for quantitative proteomics. *Nat. Protoc.* **4**, 484-494 (2009).

Supplementary information is linked to the online version of the paper at www.nature.com/nature.

Acknowledgements We thank Elmar Schiebel and Peng Liu for providing constructs and *Xenopus* egg extracts. We also appreciate Gislene Pierre and Wenbo Wang for providing constructs and sharing unpublished results. D.I. was supported by the Human Frontier Science Program (HFSP) long-term fellowship and the Japan Science Promotion Society (JSPS) fellowship for research abroad. O.J.G. was recipient of a start-professorship of the German excellence initiative, ZUK 49/TP1-16, as part of ZUK 49: Institutional strategy to promote top level research awarded to Heidelberg University. This project was supported by the ERC Advanced Grant - Manipulating and Imaging Stem Cells at Work (J.W.).

Author contributions O.J.G. supervised the project. D.I. and O.J.G. conceived and designed the project with critical input from J.W. D.I. performed all the experiments and analysed the data. M.S. and T.T established CRISPR-Cas9 system. D.I. and O.J.G. wrote the manuscript. J.W. supervised and supported D.I.

Author information The authors declare no competing financial interests. Reprints and permissions information is available at www.nature.com/reprints.

Correspondence and request for materials should be addressed to O.J.G. (o.gruss@zmbh.uni-heidelberg.de) and D.I. (daigo.inoue@cos.uni-heidelberg.de).

Figure legends

Figure 1 | Abnormal cleavage divisions of Wdr8$^{-/-}$ zygotes are rescued by EYFP-huWdr8 expression. a, Phenotypes of paternal and maternal Wdr8$^{-/-}$ embryos before and after midblastula transition (MBT). The maternal Wdr8$^{-/-}$ embryos, but not the paternal, showed disordered cleavage divisions and failure of gastrulation. **b,** Timing of cleavage cycles in Wdr8$^{-/-}$ and wild-type specimens. Data represents median with minimum to maximum. Total embryos, 10 (Cont.), 11 (Wdr8$^{-/-}$). **c, d,** Full rescue of Wdr8$^{-/-}$ zygotes by exogenous expression of EYFP-huWdr8 (**c**) and its efficiency at St.20 (**d**). n, total embryos from three independent experiments. Data represent mean ± s.e.m. Scale bars, 200 μm.

Figure 2 | Wdr8 localises to the centrosome in the rescued Wdr8$^{-/-}$ blastomeres. a, b, Spatiotemporal localisation of EYFP-huWdr8 in the rescued Wdr8$^{-/-}$ zygotes. Time-lapse images show stereotypic centrosome cycles from one- to 4-cell stage (**a**) and 8-cell stage (**b**). Time, min. **c, d,** Wdr8 is a novel centrosome protein. EYFP-huWdr8 colocalised with γ-tubulin and PCM1 (**c**), resembling the wild-type situation (**d**). Scale bars, 100 μm (**a**), 200 μm (**b**), 10 μm, (**c**, **d**).

Figure 3 | Centrosome and spindle abnormalities in Wdr8$^{-/-}$ blastomeres. a, b, Abnormal PCM and mitotic spindle assemblies in Wdr8$^{-/-}$ blastomeres. In comparison with wild-type (Fig. 2d), Wdr8$^{-/-}$ eggs exhibited severely scattered γ-tubulin/PCM1 (**a**) and multipolar mitotic spindles (**b**) together with aneuploidy at metaphase (**a**, **b**). These abnormalities were fully rescued by EYFP-huWdr8 expression (Fig. 2c, Fig. 3b). Scale bars, 10 μm.

Figure 4 | WD40 domains are essential for Wdr8 function. a, The conserved four WD40 domains in huWdr8. Mutations for WD mutant variants are denoted in red. **b,** External phenotypes of WD mutant-injected Wdr8$^{-/-}$ embryos. Note that both variants mostly localised in the cytoplasm, unable to rescue Wdr8$^{-/-}$ embryos. **c,** Time-lapse

644 images of EYFP-196/197AA localisation in Wdr8$^{-/-}$ blastomeres. EYFP-196/197AA
645 weakly localised in the centrosome with multiple foci, which disappeared during
646 cleavages. Time, min. **d, e,** Both mutant variants expression were unable to rescue
647 abnormal PCM assembly (γ-tubulin/PCM1), multipolar mitotic spindles, and
648 aneuploidy. Scale bars, 200 μm (**b**), 100 μm (**c**), 10 μm (**d, e**).
649 **Figure 5 | WD40 domains is essential to form Wdr8-SSX2IP complex and its**
650 **localisation. a,** Centrosome targeting of EYFP-196/197AA-PACT was insufficient
651 for centrosomal localisation and the rescue of Wdr8$^{-/-}$ embryos. **b, c,** Identification of
652 Wdr8 interaction factors by mass spectrometry and immunoblot analyses with
653 *Xenopus* egg extracts. WT, but not WD mutant variants, interacted with SSX2IP (**b, c**).
654 Contrary, γ-TuRC subunits/Nedd1 (**b**) and γ-tubulin (**c**) interacted with Wdr8
655 independently of WD40 domains. *, background. **d,** Interdependent localisation of
656 Wdr8 and SSX2IP via WD40 domains. Due to failure of Wdr8-SSX2IP interaction,
657 EYFP-196/7AA, but not WT, was unable to colocalised with SSX2IP to the
658 centrosome in Wdr8$^{-/-}$ blastomeres. **e,** Wdr8-SSX2IP localises to the centrosome by
659 tethering PCM components (e.g. γ-TuRC, which is essential for maternal PCM
660 assembly). The absence of maternal Wdr8 or dysfunction of its WD40 domains
661 causes PCM assembly defects. Scale bars, 200 μm (**a**), 20 μm (**d**).
662
663 **Extended Data Figure and Supplementary information legends**
664 **Extended Data Figure 1 | CRISPR-Cas9 mediated knockout strategy to generate**
665 **Wdr8$^{-/-}$ medaka line. a,** A sgRNA was designed to knockout (KO) exon-3 of
666 OlWdr8 by inserting 5' homology flank (HF) and GFP with a stop codon (see details
667 in Methods). **b,** The screening of Wdr8$^{-/-}$ fish by genotype PCR. Two sets of primers,
668 Ex1_F-T31_R and Ex1_F-GFP_R, were used to detect wild-type and the KO genomic

669 locus, respectively. Note that WT locus was detected from genomic DNAs of WT and
670 Wdr8$^{-/+}$, but not that of Wdr8$^{-/-}$. On the other hand, the KO locus was detected from
671 genomic DNAs of Wdr8$^{-/+}$ and Wdr8$^{-/-}$, but not that of WT, due to the presence of
672 GFP insertion.

673 **Extended Data Figure 2 | External phenotype of Cab wild-type and Wdr8$^{-/-}$**
674 **hatchlings (F3 generation, see Methods).** Wdr8$^{-/-}$ hatchlings rescued by maternal
675 Wdr8 developed normally with no obvious external abnormalities, comparable to
676 wild-type. Scale bars, 500 μm.

677 **Extended Data Figure 3 | External phenotype of the hatchling from Wdr8$^{-/-}$**
678 **father in comparison with wild-type hatchling.** As in Extended Data Figure 2, there
679 were no obvious differences, demonstrating that paternal Wdr8 is not implicated in
680 both early and later stage development of medaka. Scale bars, 500 μm.

681 **Extended Data Figure 4 | Detailed process of mitotic spindle assembly in Cab**
682 **and Wdr8$^{-/-}$ blastomeres.** Whereas bipolar mitotic spindle was faithfully formed
683 from prometaphase to telophase in wild-type blastomeres, fragmented centrosomes
684 (PCM1) caused multipolar spindles as well as severe chromosome instability during
685 mitosis in Wdr8$^{-/-}$ blastomeres. Scale bars, 10 μm.

686 **Extended Data Figure 5 | Western blot analysis to compare the protein level**
687 **between EYFP-huWdr8 and EYFP-196/197AA.** Expression levels of both proteins
688 were almost equivalent, demonstrating that mutation in WD40 domain did not affect
689 on protein stability.

690 **Extended Table 1 |** The chosen Wdr8-sgRNA target site has only two potential off-
691 target sites in the entire medaka genome. Search-parameters (see [40] for further
692 details): core length = 12, max. core mismatches = 2, max. total mismatches = 4,
693 PAM = NGG

Chromosome	start	end	strand	MM	target_seq	PAM	alignment	distance to next exon	position	gene name	gene id
	81	81									
	81	81			GGTCTCT	T	|||||||[|||		Ex		ENSOR
	46	48			CGAGCAG	G	||||||||]		on	wra	LG0000
chr7	7	9	+	0	CCGGAC	G	PAM	0	ic	p73	0004450
							||||-|--		Int		
	96	96			GGTCACA	A	[|-		ro	MA	
chr2	58	58			TGTGCAG	G	||||||||\]		ni	PK	XLOC_
3	52	74	+	4	CCGGAC	G	PAM	482	c	11	015134
							-|||-				
	22	22					|||[|||||-				
	85	85			CGTCCCT	G	|||-		Ex		ENSOR
	05	05			CGAGCAT	G	||]PA		on	csr	LG0000
chr7	30	52	-	4	CCGCAC	G	M	0	ic	np2	0015651

694

695 **SI Movie 1 | Live imaging of EYFP-huWdr8 localisation in the rescued Wdr8$^{-/-}$**

696 **embryos.** EYFP-huWdr8 localised to the one or two dots in individual blastomeres,

697 showing stereotypic centrosome cycles during embryonic cell cycles from one- to 4-

698 cell stage.

699 **SI Movie 2 | Live imaging of EGFP localisation from one- to 4-cell stage of Cab**

700 **wild-type embryos.** EGFP alone did not localise to the centrosome-like dots as

701 EYFP-huWdr8 did in Wdr8$^{-/-}$ blastomeres.

702 **SI Movie 3 | Live imaging of EGFP localisation from one- to 4-cell stage of Wdr8^{-}**

703 **$^{/-}$ embryos.** EGFP alone did not localise to the centrosome-like dots as EYFP-huWdr8

704 did in Wdr8$^{-/-}$ blastomeres. Note that Wdr8$^{-/-}$ disorderly divided blastomeres with

705 cytokinesis failure.

706 **SI Movie 4 | Live imaging of EYFP-196/197AA localisation from two-cell stage of**

707 **Wdr8$^{-/-}$ embryos.** EYFP-196/197AA mostly localised to the cytoplasm but oscillated

708 weak centrosomal localisation with multiple foci during cleavages. Note that EYFP-

709 196/197AA was not able to rescue the abnormal cleavage divisions of Wdr8$^{-/-}$

710 embryos.

Figure 1 (Inoue D. et al.)

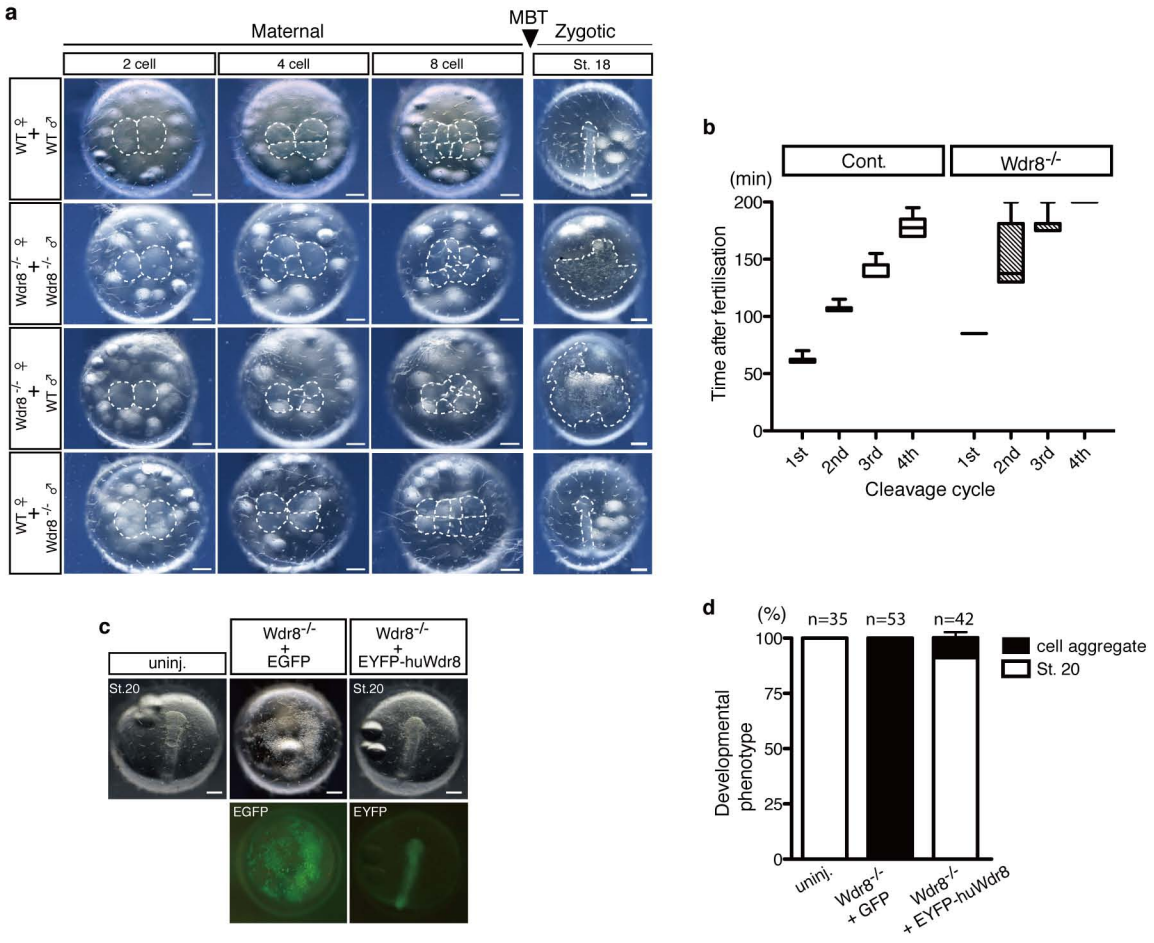

Figure 2 (Inoue D. et al.)

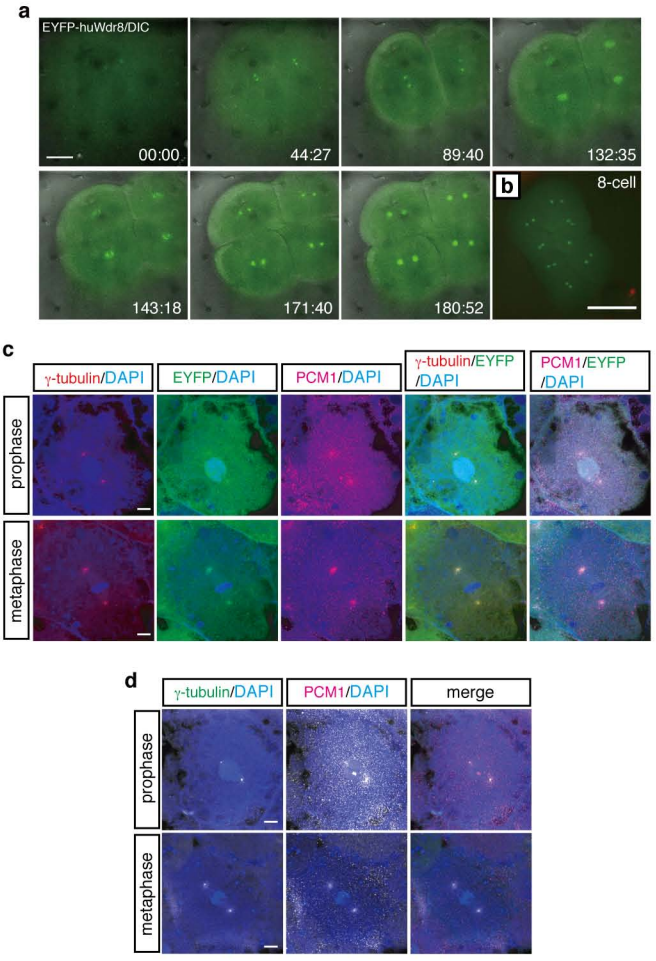

Figure 3 (Inoue D. et al.)

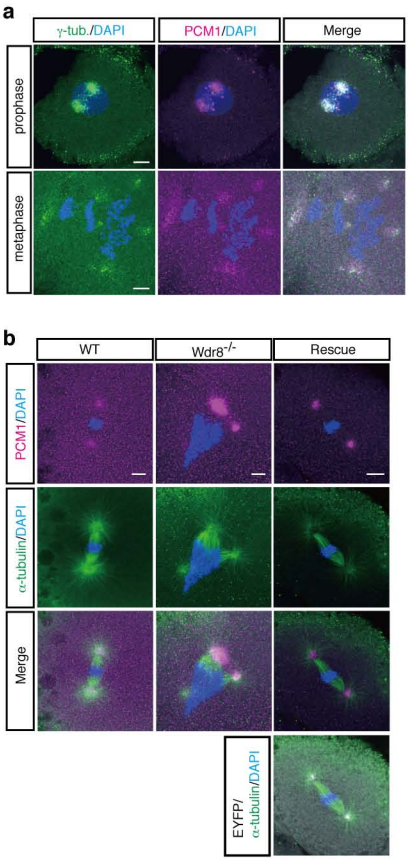

Figure 4 (Inoue D. et al.)

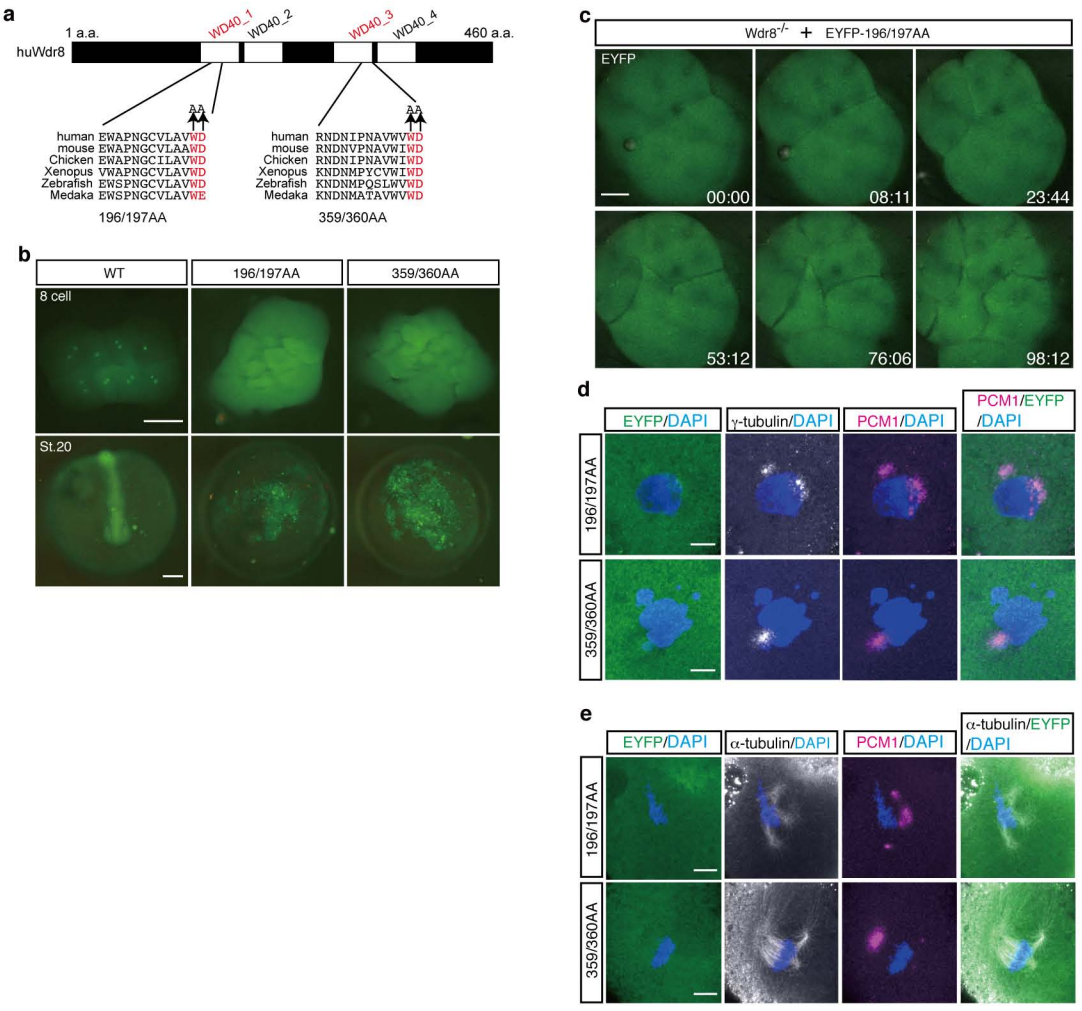

Figure 5 (Inoue D. et al.)

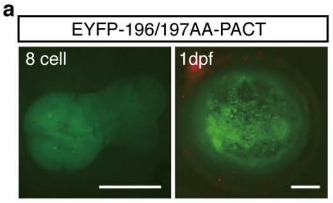

b

WD1; 196/197AA WD3; 359/360AA

protein	accession #	MW(kD)	probability (%)			unique peptides			% coverage		
			WT	WD1	WD3	WT	WD1	WD3	WT	WD1	WD3
SSX2IP	gi|147905814	64	100	6	—	2	0	—	3.7	0	—
γ-tubulin	gi|118405000	51	100	100	100	3	3	3	73	56	69
TUBGCP2	gi|148231855	60	100	100	100	23	24	26	50	55	54
TUBGCP3	gi|21362563	104	100	100	100	33	37	34	43	48	43
TUBGCP4	gi|148230420	76	100	100	100	17	20	19	39	46	43
TUBGCP5	gi|512821491	118	100	100	100	10	13	10	14	17	12
TUBGCP6	gi|148226294	184	100	100	100	19	15	17	17	14	14
NEDD1	gi|353523817	73	100	100	100	21	20	24	32	33	42

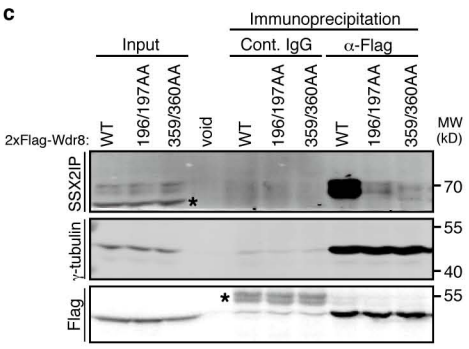

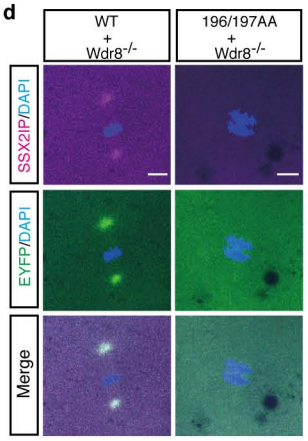

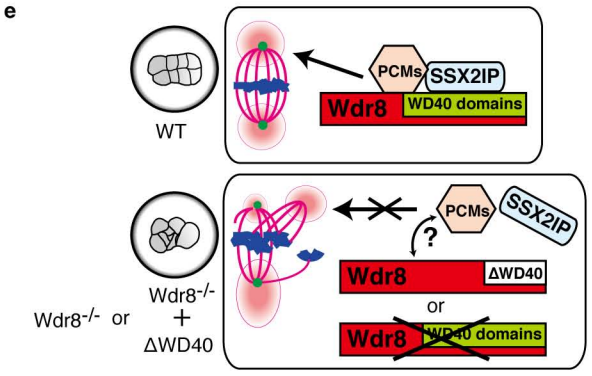

Extended Data Figure 1 (Inoue D. et al.)

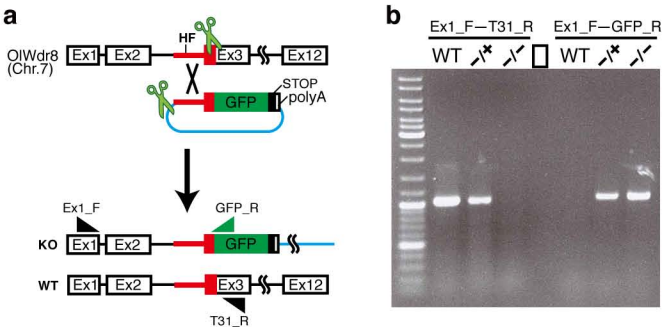

Extended Data Figure 2 (Inoue D. et al.)

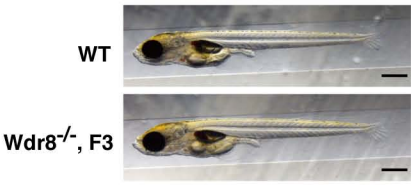

Extended Data Figure 3 (Inoue D. et al.)

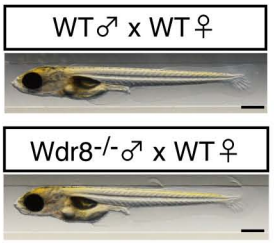

Extended Data Figure 4 (Inoue D. et al.)

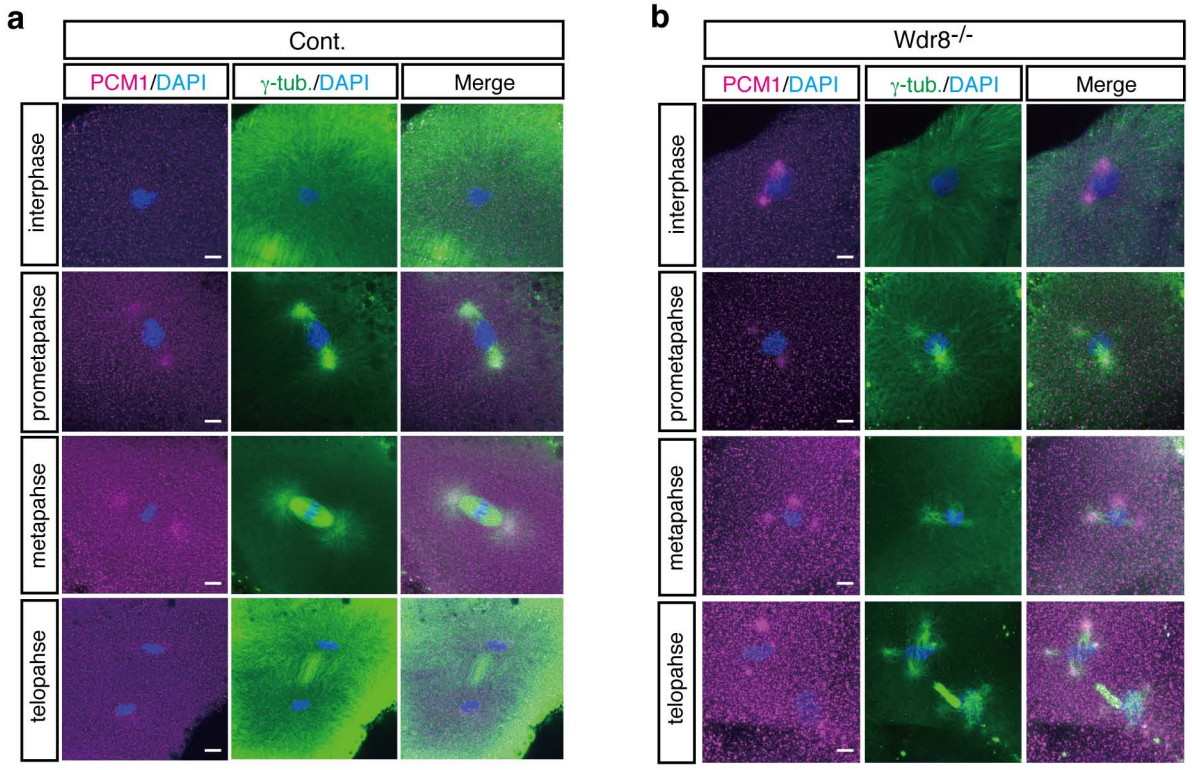

Extended Data Figure 5 (Inoue D. et al.)